

Modeling shear behavior of reinforced concrete beams strengthened with externally bonded CFRP sheets

Umair Khan^{1a}, Mohammed A. Al-Osta^{1b} and A. Ibrahim^{*2,3}

¹Civil and Environmental Engineering Department, King Fahd University of Petroleum and Minerals (KFUPM), Dhahran, Saudi Arabia

²Department of Civil Engineering, University of Idaho, Moscow, Idaho, 83844, USA

³Structural Engineering Department, Faculty of Engineering, Zagazig University, Egypt

(Received April 6, 2016, Revised August 25, 2016, Accepted September 25, 2016)

Abstract. Extensive research work has been performed on shear strengthening of reinforced concrete (RC) beams retrofitted with externally bonded carbon fiber reinforced polymer (CFRP) in form of strips. However, most of this research work is experimental and very scarce studies are available on numerical modelling of such beams due to truly challenging nature of modelling concrete shear cracking and interfacial interaction between components of such beams. This paper presents an appropriate model for RC beam and to simulate its cracking without numerical computational difficulties, convergence and solution degradation problems. Modelling of steel and CFRP and their interfacial interaction with concrete are discussed. Finally, commercially available non-linear finite element software ABAQUS is used to validate the developed finite element model with key tests performed on full scale T-beams with and without CFRP retrofitting, taken from previous extensive research work. The modelling parameters for bonding behavior of CFRP with special anchors are also proposed. The results presented in this research work illustrate that appropriate modelling of bond behavior of all the three types of interfaces is important in order to correctly simulate the shear behavior of RC beams strengthened with CFRP.

Keywords: reinforced concrete beams; CFRP; shear behavior; bond behavior; finite element method

1. Introduction

Concrete structures require retrofitting due to number of reasons which may include deficiencies either in the design or construction practices, deterioration due to adverse environmental conditions or overuse of structure in its useful life.

In modern structural engineering, carbon fiber reinforced polymers is very common solutions for strengthening and retrofitting of deficient concrete structures, Lima (2016). Due to its inherent advantages including light weight which makes it easy to handle, high strength about five times higher the structural steel, and corrosion resistance which increases useful lifetime of structures and is also highly versatile in application. The most common configurations include side wrap, U-shaped and full wrapping for shear strengthening and bottom wrap is most common for flexural strengthening and retrofitting (Panjehpour, Ali *et al.* 2014, Prem *et al.* 2016). Experimental studies on laboratory scale samples have shown great improvements both in terms of strength enhancement and durability of concrete structures. However to use CFRP effectively in terms of strength utilization and to understand their behavior and interactions with concrete

members especially on large scale such as bridge girders there is a need to accurately simulate these experiments using a non-linear finite element method (FEM) to understand key modelling parameters influencing the results of simulation.

May be due to the fact that accurate modelling of concrete shear cracking and interfacial interactions between concrete and internal steel and with CFRP and concrete is truly of challenging nature, very limited research work on detailed finite element modelling of shear critical beams are available in the literature. In the existing research work with few exceptions like (Otoom, Smith *et al.* 2006, Smith, Otoom *et al.* 2006, Tzoura and Triantafillou 2016) tension stiffening approach is the most commonly used method to model the post-cracking behavior of concrete. Tension stiffening model numerically limits the rate of stress drop across a smeared crack once the crack is initiated, stabilizing the numerical solution: according to the ACI Committee 446 (1997), the tension stiffening method inherently embody the fracture energy therefore models based on this technique are not a true representative of fracture mechanics. Further on, among the advanced literature method regarding FRP reinforced elements, it has to be mentioned the microplane-based approach initially proposed in (Gambarelli, Nisticò *et al.* 2014) to predict the behavior of FRP confined concrete columns and then proposed in (Nisticò, Ožbolt *et al.* 2016) to simulate an experimental investigations (Bocciarelli, Gambarelli *et al.* 2014) regarding RC elements strengthened with CFRP laminates.

Therefore, for accurate modeling to represent true pre

*Corresponding author, Assistant Professor

E-mail: aibrahim@uidaho.edu

^aMS Student, E-mail: g201405540@kfupm.edu.sa

^bAssistant Professor, E-mail: malosta@kfupm.edu.sa

and post-cracking behavior of shear critical reinforced concrete beams with and without CFRP, it is necessary to adopt suitable models to simulate cracking in concrete. In addition, a bond between steel and concrete and with concrete and CFRP plays an important role on overall behavior of reinforced concrete beams. In this paper, advanced finite element models to simulate cracking in concrete are developed, discussed and adopted. The models take into account the numerical computational difficulties, convergence and solution degradation problems associated with other concrete models. Modelling of concrete, reinforcing steel and CFRP and concrete-steel and concrete-CFRP bond and contact behaviors are then discussed. Finally, the commercially available non-linear finite element software ABAQUS is used to validate the developed finite element model with key tests performed on full scale T-beams with and without CFRP retrofitting. The validation was based on the extensive experimental study "Shear Strengthening of Reinforced and Pre-stressed Concrete Beams Using Carbon Fiber Reinforced Polymers Sheet and Anchors" by Kim, Quinn *et al.* (2011). The modelling parameters for bonding behavior of CFRP with special anchors are then proposed.

2. Finite element model

Finite element model is presented below delineating the modelling to simulate shear cracking in concrete followed by modelling of reinforcing steel and CFRP and their contact behavior with concrete. Displacement control loading is applied and dynamic explicit solution approach is adopted which has a conditionally stable solution technique using explicit integration. This type of analysis was chosen because it showed stability in solving problems that are static and Quasi-static process modelling problems including complex contact (Simulia 2013). This method can be good to simulate material degradation or failure, such as cracking of concrete. Based on the literature, analysis using this method rarely encounters problems of convergence. However, for static problems using dynamic analysis, inertial effects should be minimized by using slow loading rates or by increasing the mass density so that the oscillation of the results is limited (Mercan 2011). In this study, it has been found that using loading time one second has given good results through defining two load steps (initial and dynamic explicit) with automatic increments and unlimited maximum time increments. The nonlinear finite element software ABAQUS is utilized to conduct the study and the proposed modeling parameters.

2.1 Cracking simulation in concrete

To simulate quasi-brittle nature of reinforced concrete, various conceptual models are available in literature which includes discrete crack model, smeared crack model, and inner softening band. Numerical modelling of concrete cracking is mostly carried out using discrete crack and smeared crack models such as the one proposed by Chen GM (2010). In the discrete crack model, opening which arises due to cracks are physically modelled and taken as a

geometrical identity. Since cracks are defined along the surfaces of the elements, they create mesh bias. A lot of researches attempted to resolve this issue by developing finite element codes capable of generating re-meshing like Yang (2003, 2004, 2005) but the computational difficulties associated with re-meshing is still a great challenge as found by De Borst, Remmers *et al.* (2004). While in the case of smeared crack models, a phenomenon known as "strain localization" leads to zero energy utilization during crack opening when element size approaches zero, this results in a non-mesh objective case that causes solution not to converge or material to degrade.

In this paper, damage plasticity model has been utilized for concrete which is a constitutive model available in the ABAQUS material library. In the damage plasticity model, compression and tension are two hardening variables that control development of yield surface. A continuum damage mechanism is used to model crack opening and its propagation by stiffness degradation approach which essentially means that elasticity is degraded in concrete where it cracks.

2.2 Concrete model

To model a concrete material in ABAQUS "concrete damaged plasticity" model was developed by (Lubliner, Oliver *et al.* 1989) and elaborated by (Lee and Fenves 1998). The model is used which requires the following material functions:

- Uniaxial stress-strain relation of concrete under compressive and tensile loading.
- Damage parameters d_c and d_t for compressive and tensile load, respectively. These parameters could be used to identify and validate damage pattern of the developed model and compare it with experimental work.

Tsai (1998) stress-strain relationship has been adopted in this paper. The model has advanced empirical parameters to control the ascending as well as post-peak behavior of stress-strain curve for unconfined concrete. The constitutive concrete law introduced by Tsai (1998) was used to define properties like elastic modulus, compressive and tensile strength history, and to be used in Eqs. (7) and (8). The stress-strain relationship is as follow

$$y = \frac{mx}{1 + \left(m - \frac{n}{n-1}\right)x + \frac{x^n}{n-1}} \quad (1)$$

where y is ratio of concrete stress to the ultimate strength and given by

$$y = \frac{f_c}{f'_c} \quad (2)$$

" x " is the ratio of concrete strain to the strain at y equals unity

$$x = \frac{\epsilon}{\epsilon_c} \quad (3)$$

" m " is ratio of initial tangent modulus to secant modulus at y equals unity

Table 1 Concrete parameters used in the plastic damage model

Concrete Strength (MPa)	Mass Density (ton/mm ³)	Young's Modulus (MPa)	Poisson's Ratio	Dilation Angle ψ (Degrees)	Eccentricity ϵ	$f_{bo}f_{co}$	b_c/b_t
Varies	2.4E-009	26764.7	0.2	36	0.1	1.16	0.7

$$m = \frac{E_o}{E_c} \quad (4)$$

“ n ” is a steepness rate control factor for post-peak part of stress-strain relation.

The factors “ m ” and “ n ” can be expressed as

$$m = 1 + \frac{17.9}{f'_c \text{ (MPa)}} \quad (5)$$

$$n = \frac{f'_c}{6.68 \text{ (MPa)}} - 1.85 > 1 \quad (6)$$

Concrete compression damage parameter that is used in the proposed model is given by (Birtel and Mark 2006)

$$d_c = 1 - \frac{f_c E_c^{-1}}{\epsilon_c^{pl} \left(\frac{1}{b_c} - 1 \right) + f_c E_c^{-1}} \quad (7)$$

where

d_c = Concrete compression damage parameter

f_c = Compressive Stress

E_c = Modulus of elasticity of concrete

ϵ_c^{pl} = Plastic strain corresponding to compressive strength

b_c = Constant ranges $0 < b_c < 1$

Whereas concrete tension damage parameter is (Birtel and Mark 2006)

$$d_t = 1 - \frac{f_t E_c^{-1}}{\epsilon_t^{pl} \left(\frac{1}{b_t} - 1 \right) + f_t E_c^{-1}} \quad (8)$$

where

d_t = Concrete tension damage parameter

f_t = Tensile Stress

E_c = Modulus of elasticity of concrete

ϵ_t^{pl} = Plastic strain corresponding to tensile strength

b_t = Constant ranges $0 < b_t < 1$

The concrete parameters used in the plastic damage model are shown in Table 1.

2.3 Modelling of reinforcing steel and CFRP and their bond with concrete

Reinforcing steel has been modelled using a 2-noded linear 3-D truss element: 1) the stress- strain curve adopted for steel is elastic-perfectly plastic, 2) the other parameters used to define reinforcing steel behavior are shown in Table 2.

Table 2 Parameters of reinforcing steel

Elastic Modulus (MPa)	200,000
Poisson's ration	0.3
Mass Density (tonne/mm ³)	7.85E-009
Yield Stress (MPa)	414/517

Table 3 Unidirectional properties of CFRP used to model the lamina

Type	Thickness (mm)	Elastic Modulus (MPa)	Ultimate Strain (mm/mm)	Ultimate Stress (MPa)
CFRP	0.508/	56537/	0.01/0.0105	565/903
B/A	0.279	86874		

*A and B are different CFRP laminates

Steel reinforcement is bonded with concrete as an embedded element in ABAQUS. Embedment technique successfully used by many researchers and considered a very powerful finite element tool which allows number of elements to be embedded inside another element which known as host element. One of the significant utilization of embedment technique is the modelling of interaction surface between the embedded and the host element, which eradicates numerical costly iterations linked with surface formulations. CFRP has been modelled as a composite lamina in ABAQUS. The properties of CFRP used to model the lamina as linear elastic material are shown in Table 3.

The bond between CFRP and concrete is considered as perfect cohesive bond with dry contact due to the presence of anchors at the ends of each CFRP strip to avoid its premature failure by de-bonding. This assumption has been validated with study of different geometric and material parameters of the beams under consideration. The details of anchors are discussed in section 3 of this paper. Two interfacial regions were included in this model to define interaction between concrete and CFRP. The interaction between CFRP and concrete is considered as Tie (perfect) bond in region of anchor at the end of each CFRP strip to avoid its premature failure whereas the Surface-based cohesive model is used to model the bond between concrete and CFRP in all other regions as shown in Fig 1. This model input default parameters were taken as $k_{nm}=9.3$ GPa/mm (normal stiffness), $k_{ss}=11.1$ GPa/mm, and $k_{tt}=11.1$ GPa/mm (tangential directions stiffness) that define the cohesive interaction and reflects the behavior of adhesive material between concrete and the rest of CFRP strip. Since the information about the adhesion materials is not available, a default contact enforcement method in ABAQUS was adopted. Cohesion contact is employed between concrete and CFRP for interaction, which surely presume bond deterioration occurs due to stiffness degradation. This phenomena is not considered because the complete de-bonding of CFRP from concrete achieved with ultimate stress state due to the presence of CFRP anchors at the end of each strip.

3. Outline of experimental test program

Two groups of full scale experimentally tested beams

Table 4 Geometrical and material properties of test specimens

Group	Group 1		Group 2	
Specimen	24-3-2	24-3-5	48-3-1	48-3-2
Compressive Strength f'_c, MPa	24.8	24.1	26.9	26.9
Beam Dimensions				
Height h, mm	610		1220	
Span L, mm	4875		8433	
Shear span S, mm	1727		3353	
Web width b_w , mm	356		356	
Flange width b_f , mm	711		533	
Steel Reinforcement				
Tension bars	10 # 9		12 # 10	
Yield strength of tension bars f_{yt} , MPa	517		514	
Compression bars	5 # 9		6 # 9	
Yield strength of compression bars f_{yc} , MPa	414		414	
Stirrups	#3 @	254 mm	#3 @	457 mm
Yield strength of stirrups f_{yy} , MPa	414		414	
Elastic modulus of all reinforcement E_s , MPa	200,000		200,000	
CFRP				
Configuration	None	U-strips	None	U-strips
Laminate		B		A
Number of anchors/strip		1		2
Nominal thickness t_f , mm		0.508		0.279
Strip width w_f , mm		127		254
Clear spacing s_f , mm		127		254
Ultimate Stress f_f , MPa		565		903
Ultimate Strain ϵ_{uf} , mm/mm		0.01		0.0105
Elastic modulus E_f , MPa		56537		86874

wide at 254 mm center to center. In this group one anchor at the end of each CFRP strip is used to ensure the appreciable utilization of CFRP strength capacity. In-group 1, beams are tested upside down. Group 2 consists of two beams that are control beam and CRRP retrofitted beam. Each beam is 1220 mm deep and 8433 mm long with shear span to depth ratio equals to 3. The CFRP strips used to strengthen a beam are 254 mm wide at 508 mm center to center. In this group, two anchors at the end of each CFRP strip is used to ensure the appreciable utilization of CFRP strength capacity similar to group one. The reinforcement details, CFRP application, test configurations and CFRP anchors are as shown in Figs. 2-4 by Kim, Quinn *et al.* (2011).

Geometrical and material properties of test specimens categorized as group 1 and group 2 are summarized in Table 4.

4. Validation of finite element model

The proposed finite element model has been validated with four full scale experimentally tested beams as described in section 3 which includes both control and retrofitted beam specimens. The failure mode of control beams is happened due to diagonal tension crack (shear failure) whereas in retrofitted beams, failure is caused due

to rupture of CFRP strips by virtue of special CFRP anchors installed at the end of each CFRP strip. The anchors allow appreciable utilization of CFRP strength capacity without failure by de-bonding. A comparison of full scale experimentally tested beams and finite element model prediction is presented next to validate and calibrate the competency of FEM to envisage the failure load, mode of failure and overall behavior of control and retrofitted beams under shear.

4.1 Method of extracting shear contributions

Shear contribution of each stirrup passing the diagonal shear crack was calculated as follow

$$F_s = A_s E_s \epsilon_s \quad \epsilon_s \leq \epsilon_y \quad (9)$$

$$\text{and } F_s = A_s F_y \quad \epsilon_s > \epsilon_y \quad (10)$$

where F_s is the shear force resisted by each stirrup, A_s is the cross sectional area of the stirrup, E_s is the elastic modulus of steel, ϵ_s is the strain being evaluated in stirrup, ϵ_y is the yield strain of steel and F_y is the yield strength. Shear contribution of CFRP strip passing diagonal shear crack was calculated as

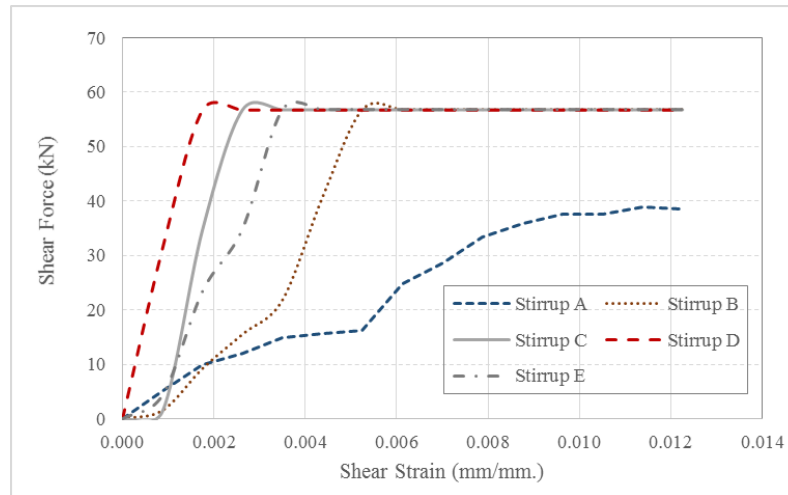


Fig. 5 Individual stirrups contribution to shear force vs. deformation response (24-3-2)

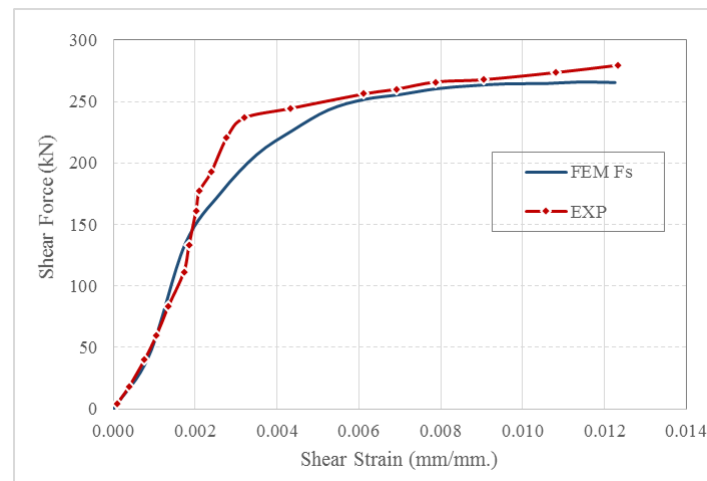


Fig. 6 Total stirrups contribution to shear force vs. deformation response (24-3-2)

$$F_f = w_f t_f E_f \epsilon_f \quad (11)$$

where F_f the shear force resisted by CFRP strip, w_f is the width of CFRP strip, t_f is the thickness of CFRP strip, E_f is the elastic modulus and ϵ_f is the strain being evaluated in CFRP strip.

Thus the total shear contribution resisted by concrete can be evaluated using the following equilibrium equation

$$F_c = F - F_s - F_f \quad (12)$$

where F_c the shear force is resisted by concrete and F the total shear force applied to critical section. Concrete strains are evaluated at main diagonal shear crack.

4.2 Control beam specimen (24-3-2)

Control beam specimen (24-3-2) as tested by Kim, Quinn *et al.* (2011) was reinforced with stirrups against shear as shown in Table 4. The predicted load versus shear strain behavioral for individual stirrups by FEM is shown in Fig. 5. The FEM curve is generated by first adding the contribution of each stirrup as shown in Fig. 5 to generate their total contribution toward the beam shear strength as

shown in Fig. 6 along with the experimentally generated curve. The contribution of stirrups passing the main shear crack are then added to the concrete shear strength contribution to get the total response of beam (24-3-2). It can be seen that the results are in good agreement with the experiment as shown in Fig. 7.

It was found that ultimate test load and the corresponding experimental values are 480.4 kN and 467.0 kN, respectively which are in close agreement and they are appreciably higher than the corresponding values obtained from ACI equations. However, the strain predicted by FE analysis is 0.009 mm/mm is somewhat different from the experimental value of 0.0123 mm/mm as shown in Fig. 8.

The predicted failure mode for beam (24-3-2) is diagonal tension crack as shown in Fig. 9. The crack pattern of the experiment and FE (damage parameter) prediction is also well matched as shown in Fig. 10 where it shows the damage of concrete (red) diagonally matching the experiment. From Fig. 11, it can be observed that stirrups B, C, D and E which cross the main diagonal tension crack have yielded at the ultimate load.

4.3 Strengthened beam specimen (24-3-5)

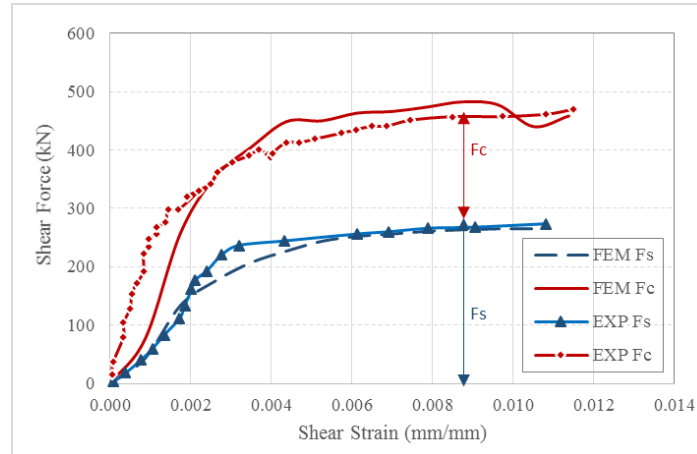


Fig. 7 Total concrete and stirrups contribution to shear force vs. deformation response (24-3-2)

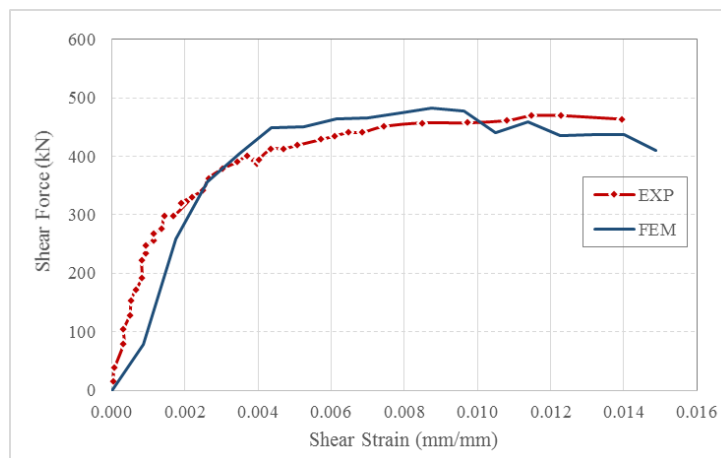


Fig. 8 Total beam shear force vs. deformation response (24-3-2)



Fig. 9 Beam (24-3-2) at failure load

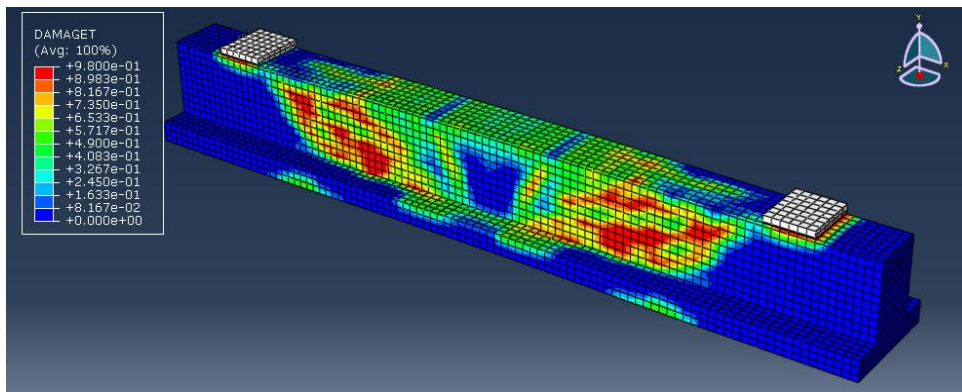


Fig. 10 FEM crack pattern of beam (24-3-2) at failure load

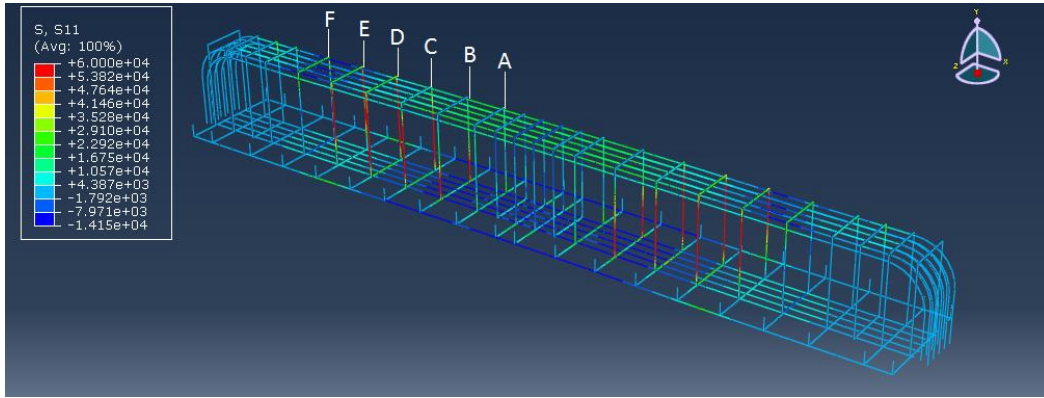


Fig. 11 Stirrups yielding state at failure load of beam (24-3-2)

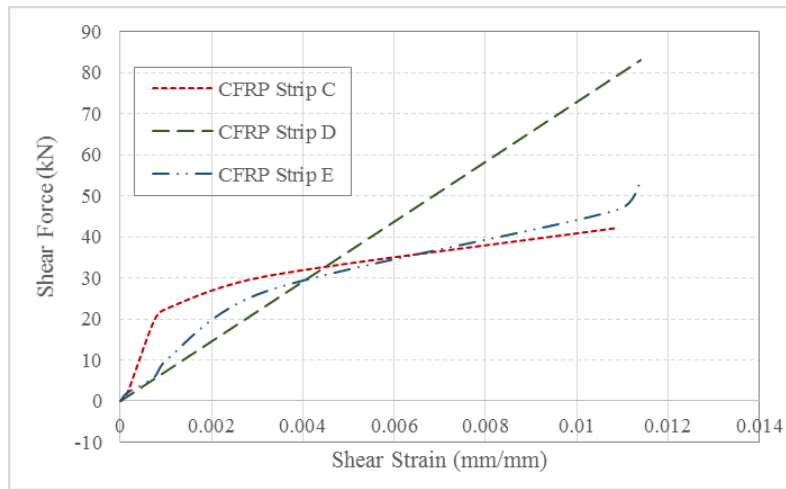


Fig. 12 Individual CFRP contribution to shear force vs. deformation response (24-3-5)

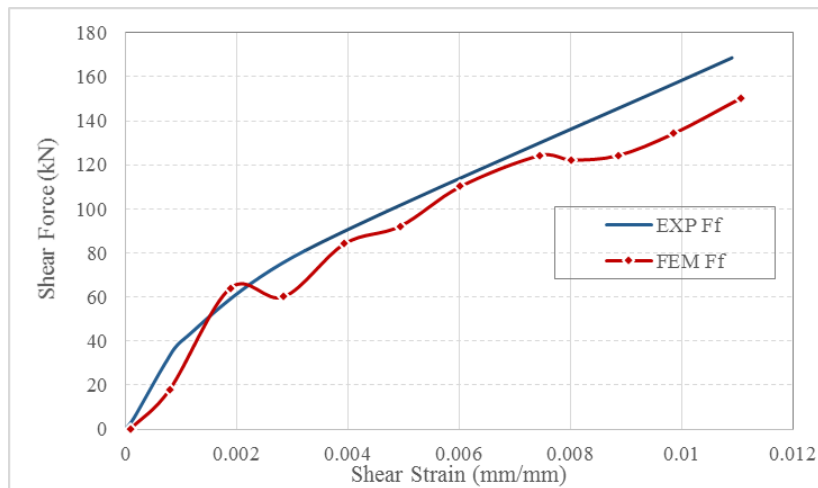


Fig. 13 Total CFRP contribution to shear force vs. deformation response (24-3-5)

The strengthened beam specimen (24-3-5) was reinforced with vertical steel stirrups and strengthened with external U-shaped CFRP strips with anchors at each end of the CFRP sheets. Adding individual contribution of CFRP strips passing the main diagonal crack is shown in Fig. 12 leading to the total contribution of CFRP as shown in Fig. 13. What was observed that strip D has a linear strength function and failed first and has a higher strength compared

to strips C and E. Similarly, individual contributions of all the stirrups passing the main diagonal crack shown in Fig. 14 are added to get total stirrups shear strength shown in Fig. 15. FE prediction of total stirrups capacity was 262 kN which is in good match with experimental corresponding value of 240.2 kN, towards the ultimate capacity of the tested beam (24-3-5). It can be seen in Fig. 15 that the shear strength of the FE predicted higher load compared to the

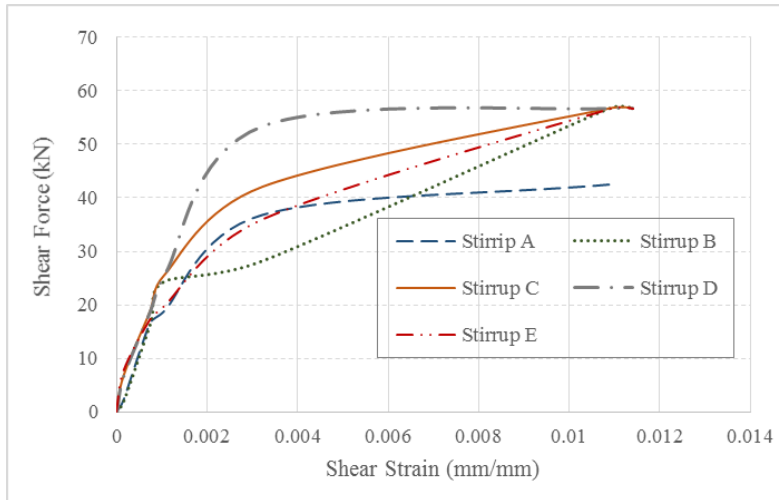


Fig. 14 Individual stirrups contribution to shear force vs. deformation response (24-3-5)

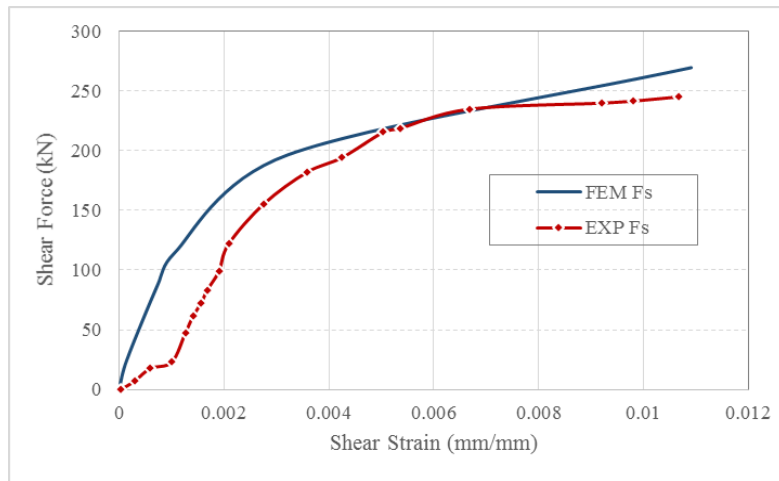


Fig. 15 Total stirrups contribution to shear force vs. deformation response (24-3-5)

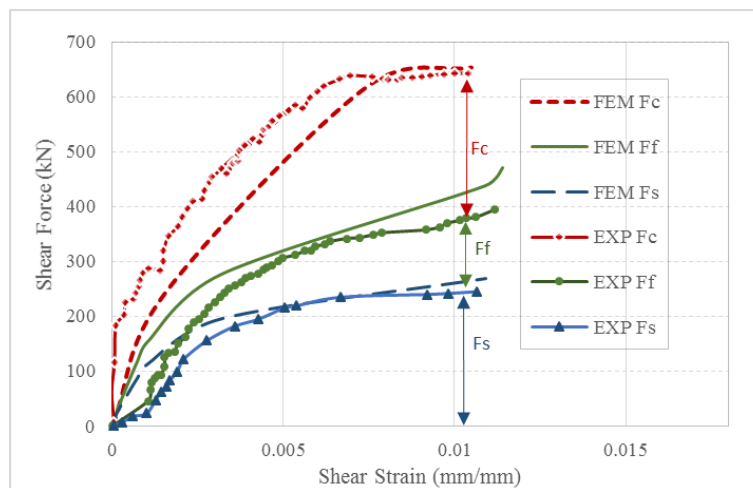


Fig. 16 Component contribution to shear force vs. deformation response (24-3-5)

experiment throughout the loading history. The concrete contribution according to the FE analysis is 262.4 kN which is 1.6% lower than the corresponding experimental value of 266.8 kN.

Shear deformation behavior of concrete, vertical

stirrups, and the carbon fibers obtained from the FE analysis and the tested beams are in acceptable agreement as shown in Fig. 16. The results are then compared with ACI shear prediction equations as shown in Tables 5 and 6 and it is found that these values are on the higher side compared to

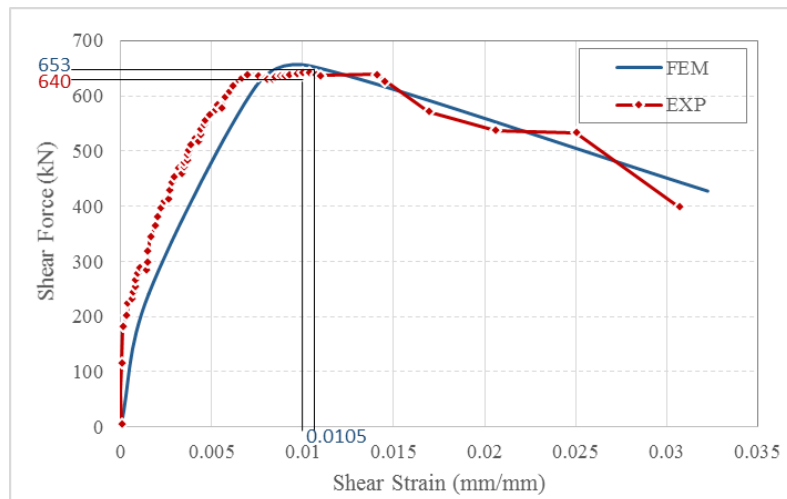


Fig. 17 Beam shear force vs deformation response (24-3-5)

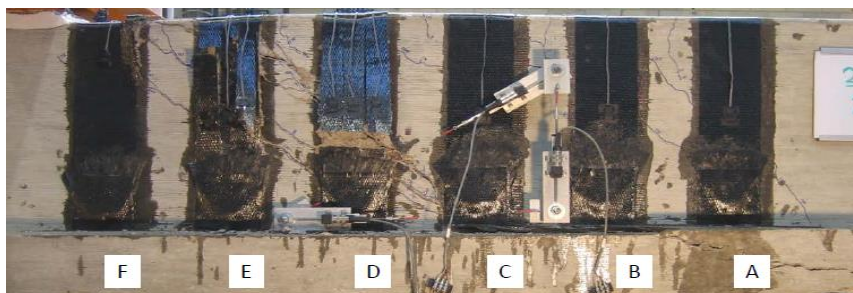


Fig. 18 CFRP rupture and concrete crack pattern (24-3-5) at failure load

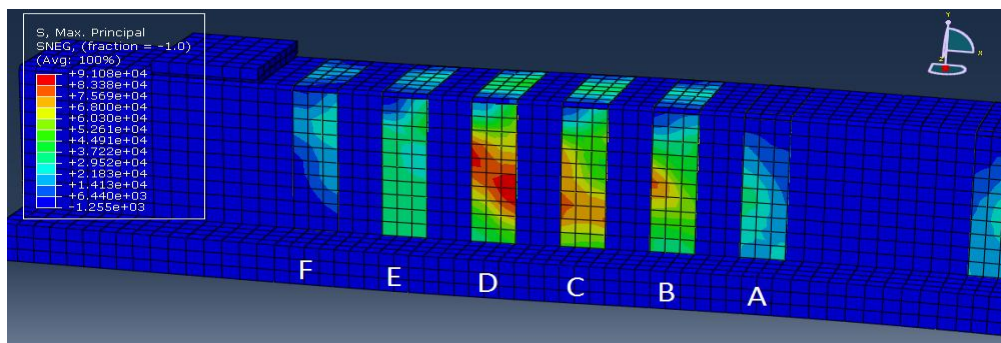


Fig. 19 FEM CFRP failure of (24-3-5) at failure load

the corresponding ACI values.

The overall shear strength of beam (24-3-5) as predicted by the FE and the experimental testing is shown in Fig. 17. The ultimate load capacity predicted by the FE is 653.8 kN whereas the corresponding experimental value is 640.9 kN. Strains obtained from FE throughout the load history is slightly higher than the corresponding values from the experiment at same shear force value. This behavior is attributed to one or more of the following reasons. First, The FE modelling is performed using dynamic explicit approach that capture the dynamic effect and the corresponding strain amplifications which is not possible to quantify in static measurement environment of an experiment. Second, typical electrical strain gauges employed in the experimental testing measures the average strain over length and can omit maximum strain in that

vicinity. Finally, as the strain gauges are positioned at some spacing from each other they can miss the point of maximum strain.

Figs. 18 and 19 show the comparison of failure modes of FE analysis with the experimental results. The FE predicted failure mode which was dominant by the rupture of strip D when it reaches a failure stress of 56537 MPa as shown in Fig. 18. The crack patterns in concrete before and after the failure of CFRP is shown in Figs. 20 and 21, respectively and are comparable with experimental crack pattern shown in Fig. 18.

Control beam specimen (48-3-1) of group 2 is reinforced with vertical steel stirrups against shear as shown in Table 4. During the experimental testing of the beam (48-3-1), the load was stopped at 653.8 kN when hair line cracks started and developed as shown in Fig. 23. To avoid excessive

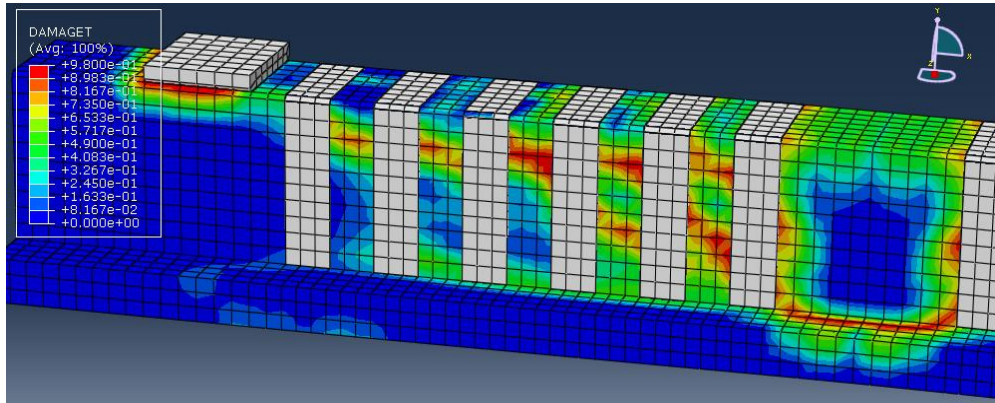


Fig. 20 FEM crack pattern in concrete (24-3-5) before CFRP rupture

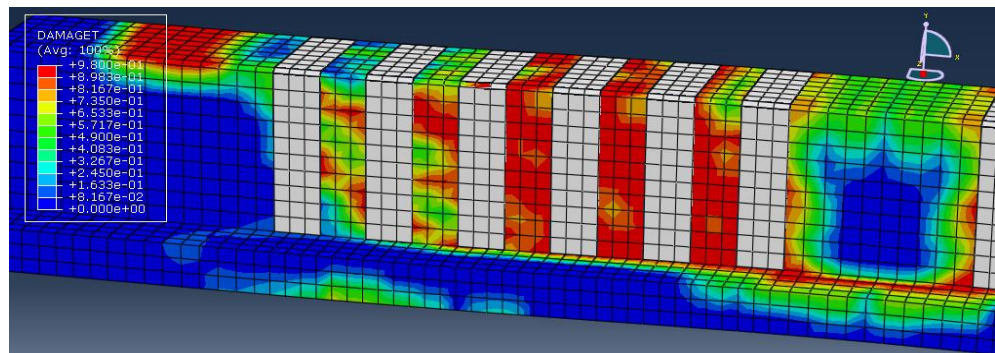


Fig. 21 FEM crack pattern in concrete (24-3-5) after CFRP rupture

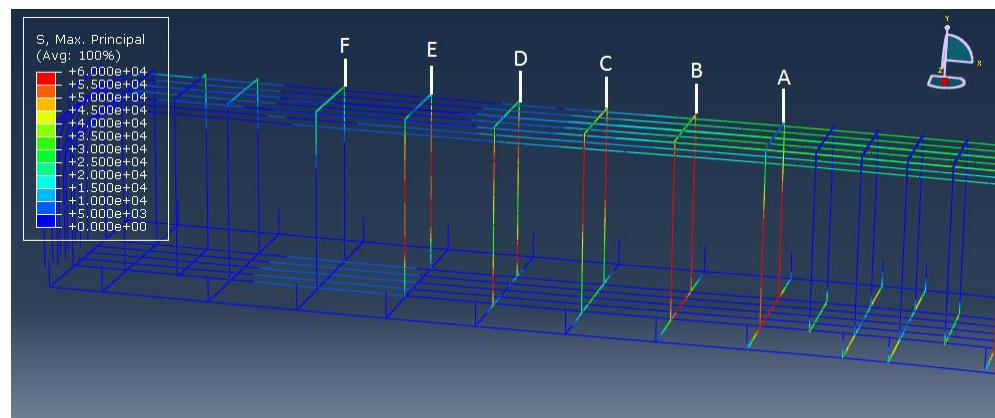


Fig. 22 Stirrups yielding state at failure load (24-3-5)

damage, the other end of same beam was then strengthened with CFRP for the test beam quoted as (48-3-2) and detailed in Table 4. In the FE analysis, beam (48-3-1) was subjected to ultimate shear capacity that was found to be 818.4 kN. The ratio of ACI equation shear capacity to the FE analysis was found to be 1.68 for the beam (24-3-2), the capacity of beam (48-3-1) comes out to be 800.6 kN which is in good agreement with the 818.4 kN shear capacity obtained from the experiments. The predicted load versus shear strain behavioral curve by FEM and experiment is shown in Fig. 23 and it is observed that deformational behavior is in good agreement up to shear value of 653.8 kN. Figs. 24 and 25 show a diagonal shear crack pattern as observed in experiment and predicted by FE analysis, respectively.

From the Fig. 22, it can be observed that stirrups A, B,

C, D and E which crosses the main diagonal tension crack have reached their yield strength of 414 MPa at the failure load.

4.3 Control beam specimen (48-3-1)

In Fig. 26, alphabets showing the position of stirrups, and it can be observed that diagonal crack is passing through stirrups B, C, D and E. The same behavior can be observed in Fig. 26 where these stirrups yielded at the ultimate load.

4.4 Strengthened beam specimen (48-3-2)

The strengthened beam specimen (48-3-2) of the second

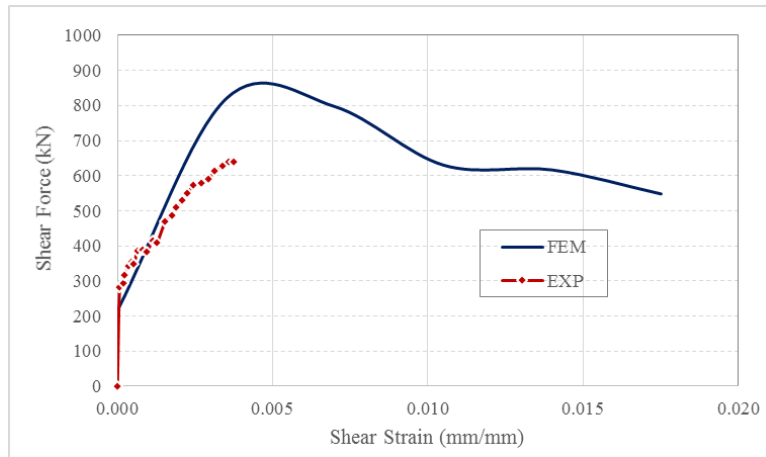


Fig. 23 Beam shear force vs. deformation response (48-3-1)

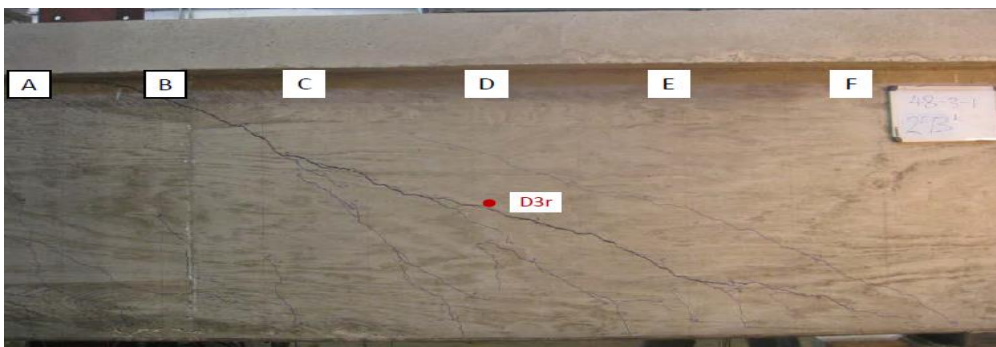


Fig. 24 Beam (48-3-1) at load of 654 KN

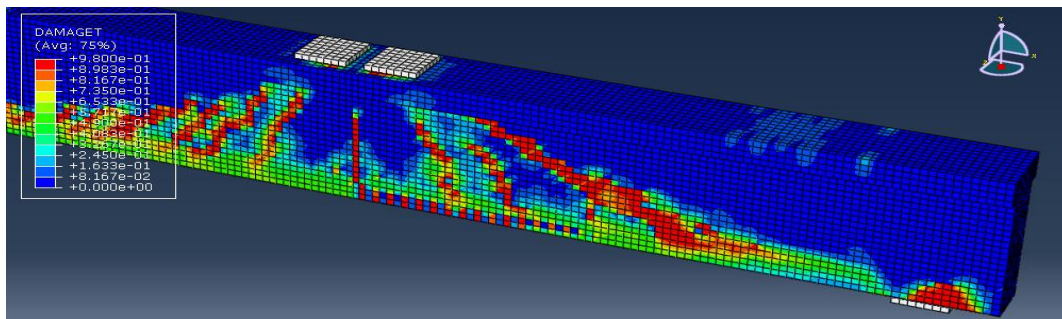


Fig. 25 FEM crack pattern of (48-3-1) at failure load

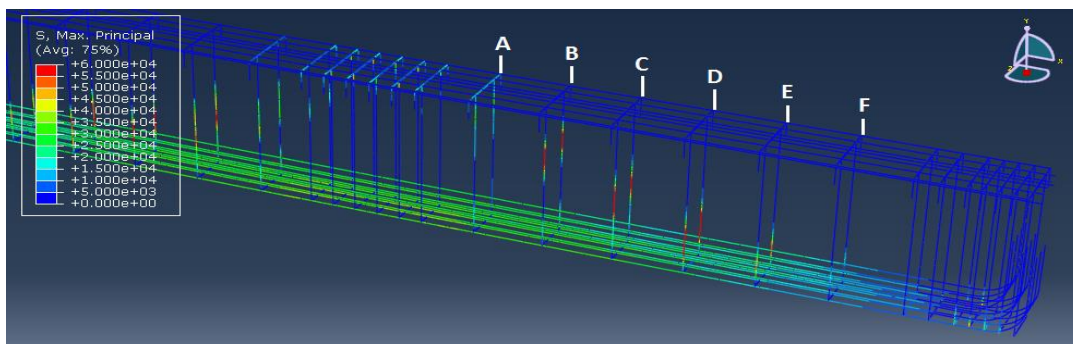


Fig. 26 Stirrups yielding state at failure load (48-3-1)

group was reinforced with steel stirrups and strengthened with external U-shaped CFRP strips with two anchors at each end of the strips. The total shear strength contribution

of CFRP as shown in Fig. 28 is obtained similar to as done by (24-3-2) that is by adding individual contribution of CFRP strips B, C, D and E passing the main diagonal crack

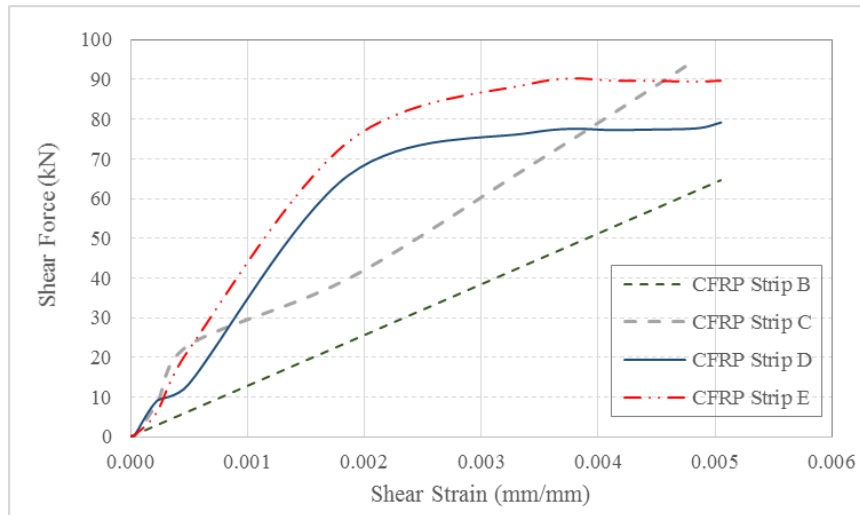


Fig. 27 Individual CFRP contribution to shear force vs. deformation response (48-3-2)

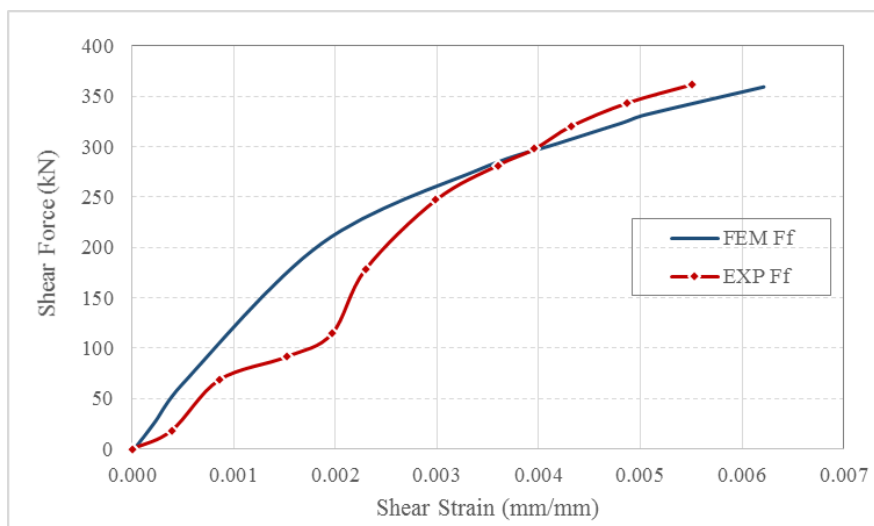


Fig. 28 Total CFRP contribution to shear force vs. deformation response (48-3-2)

as shown in Fig. 27. The ultimate shear strength of CFRP obtained from the FE analysis and the physical testing is 351.4 kN and 360.3 kN, respectively, but the overall shear deformation behavior is considerably different. This might be due to excessive slips of the CFRP strips observed in the experimental testing. The obtained curve as shown in Fig. 28 with the FE has more stiffness up to a load of 260 kN. Similarly, individual contributions of all the stirrups crossing the main diagonal cracks shown in Fig. 30 are added to get total contribution shown in Fig. 31. The FE prediction of the total capacity of stirrups is found to be 226.8 kN which is in good agreement with the corresponding experimental value of 217.9 kN, towards the total ultimate capacity of beam (48-3-2). The concrete contribution according to the FE model is 547.1 kN which is 30 % higher than the corresponding experimental value of 418.1 kN. The discrepancy between FE analysis and experimental results in terms of the concrete shear strength could be due to that same beam was loaded up to 653.8 kN which is around 80 % of its ultimate capacity (818.4 kN) during the test, this might have caused some stiffness

degradation in concrete and initial shear cracking. Contributions of each shear strength component according to the ACI equations, experiment and FE element analysis are summarized and compared in Table 5 and 6 respectively.

Shear deformation behavior of concrete, and steel stirrups from FE analysis and experiment is shown in Fig. 31.

The FE predicted failure mode observed to be due to rupture of several CFRP strips when they reach the failure stress of 90321 MPa as shown in Fig. 34, which can be compared with Fig. 33 where CFRP strip B, C and D fails at ultimate load. Figs. 33 and 35 show comparison of diagonal shear crack pattern as observed in experiment and predicted by FE analysis.

5. Evaluation of parameters to validate modelling assumption of CFRP with anchors

Different parameters related to beam geometry, reinforcement details, CFRP material, geometry of CFRP,

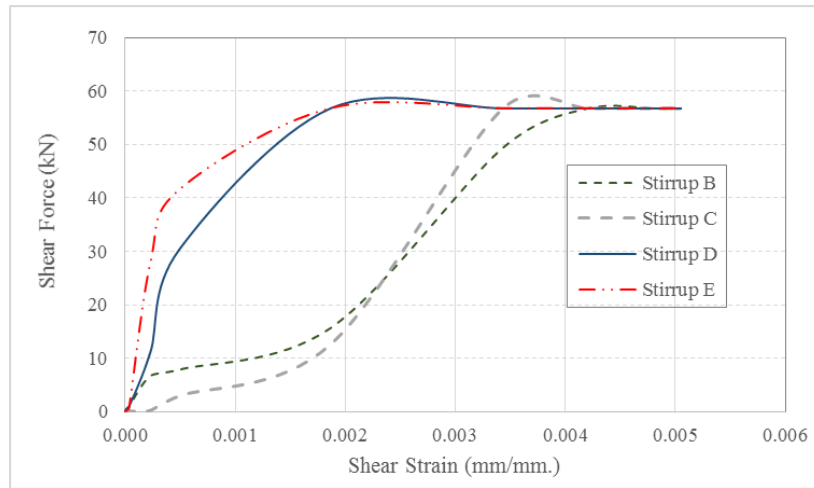


Fig. 29 Individual stirrups contribution to shear force vs. deformation response (48-3-2)

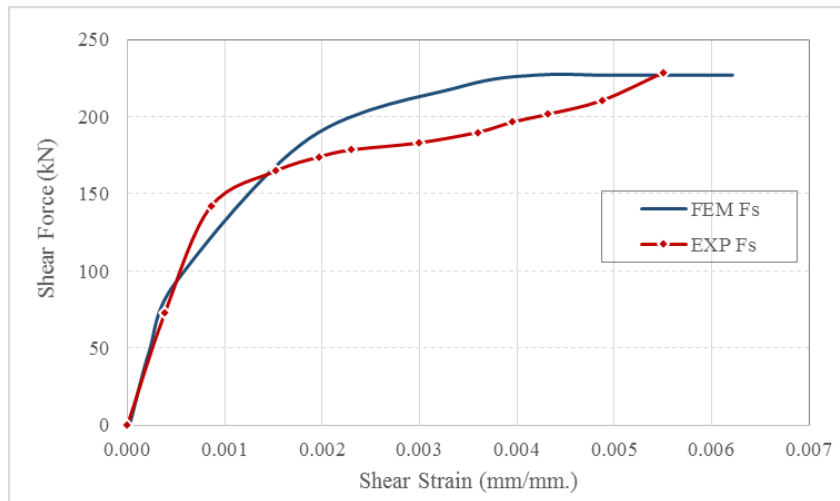


Fig. 30 Total stirrups contribution to shear force vs. deformation response (48-3-2)

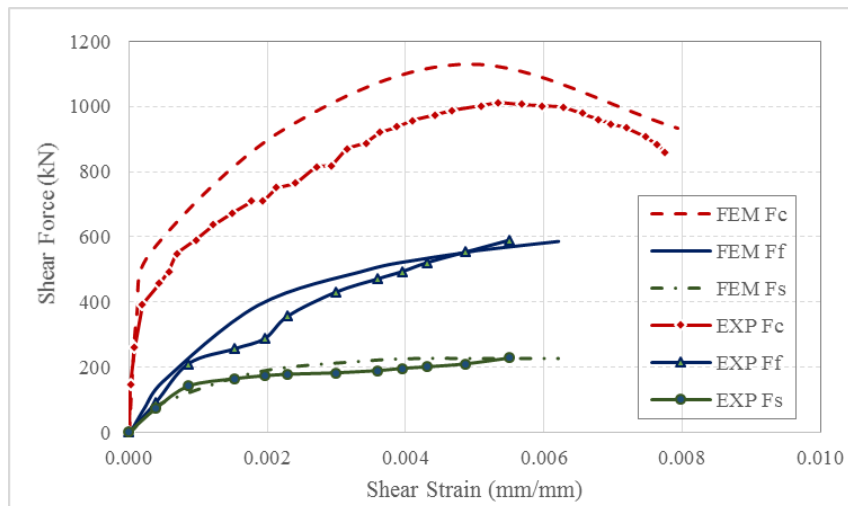


Fig. 31 Component contribution to shear force vs. deformation response (48-3-2)

spacing between CFRP strips and number of anchors considered to validate modelling assumption of CFRP anchors are discussed as follow.

5.1 Evaluation of geometric and reinforcing characteristics of RC beams

To evaluate the effect of different shear behavior of RC

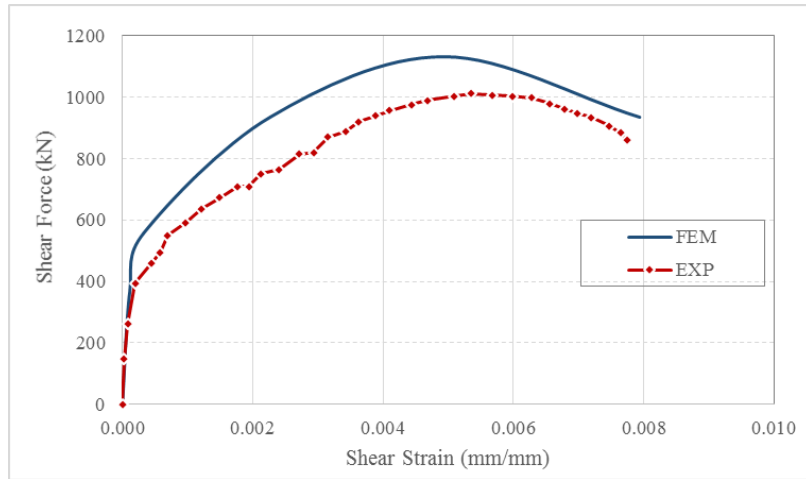


Fig. 32 Beam shear force vs deformation response (48-3-2)

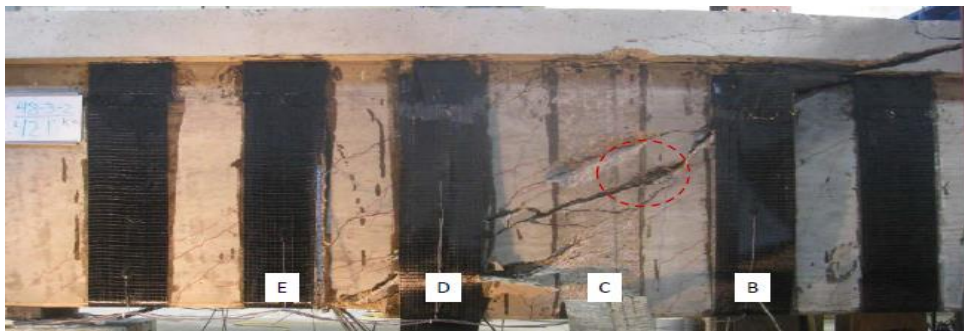


Fig. 33 CFRP rupture and concrete crack pattern (48-3-2) at failure load

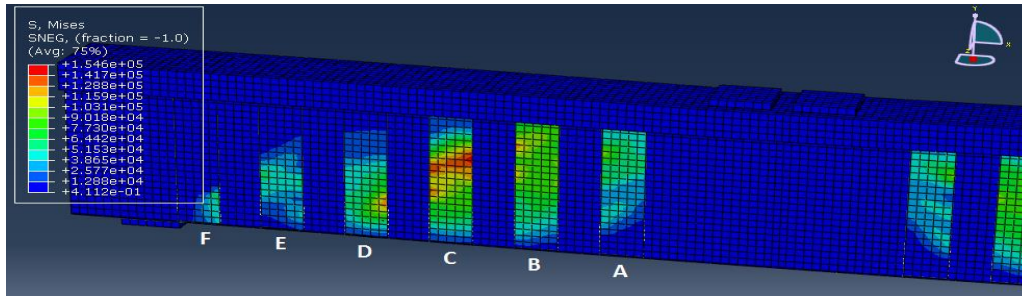


Fig. 34 FEM CFRP failure of (48-3-2) at failure load

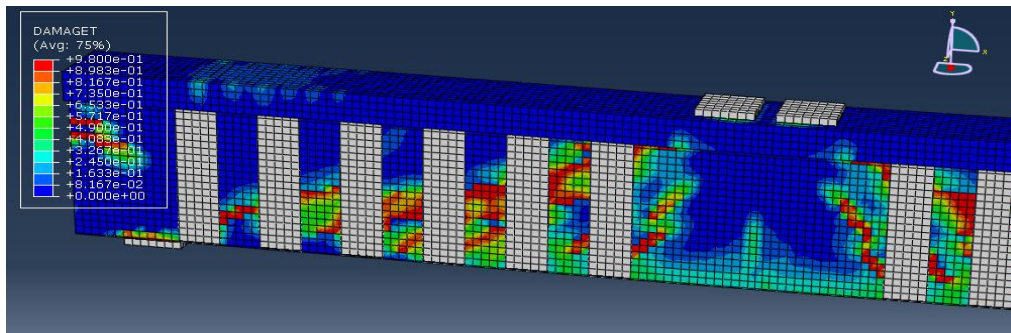


Fig. 35 FEM crack pattern in concrete (48-3-2) at failure load

beams based on the numerical modeling of CFRP with anchors, it was assumed that the contact between CFRP and concrete is considered as Tie bond in the region of anchor at the end of each CFRP strip to avoid its premature failure

whereas cohesive contact was used to simulate the behavior of adhesive material between concrete and the rest of CFRP strip.

Two groups of beams have been studied with different

Table 5 Summary of results obtained from ACI, Experiment and FE analysis

Specimen	V (kN) from ACI Eq. (α)				F (kN) from Exp. (β)				P (kN) from FEM (γ)			
	V_c^{*1}	V_s^{*2}	V_f^{*3}	V_n	F_c	F_s	F_f	F_n	P_c	P_s	P_f	P_n
24-3-2	147	138	-	285	196	276	-	467	213	267	-	480
24-3-5	142	138	111	391	267	240	138	645	227	262	165	654
48-3-1	329	147	-	476	419	235	-	654	-	-	-	818
48-3-2	329	147	267	743	431	218	351	1005	542	227	360	1130

*1 $V_c = 0.17\lambda\sqrt{f'_c} b_w d$ (ACI committee 318 2014)

*2 $V_s = \frac{A_v f_y d}{s}$ (ACI committee 318 2014)

*3 $V_f = \frac{A_{fv} f_{fe} (\sin \theta + \cos \theta) d}{s}$ (ACI Committee 440 2008)

t_f = Thickness of CFRP

$A_{fv} = 2nt_f w_f$, area of CFRP external laminates

d_f = depth of CFRP laminates

θ = angle representing the inclination of CFRP laminates

$f_{fe} = \epsilon_{fe} E_f$, effective stress in the CFRP

Table 6 Comparison of results obtained from ACI, Experiment and FE analysis

Specimen	Ratio β/α				Ratio γ/α				Ratio γ/β			
	F_c/V_c	F_s/V_s	F_f/V_f	P_c/V_c	P_s/V_s	P_f/V_f	P_n/V_n	F_n/V_n	P_c/V_c	P_s/V_s	P_f/V_f	P_n/V_n
24-3-2	1.33	1.98	-	1.65	1.45	1.94	-	1.69	1.09	0.97	-	1.03
24-3-5	1.76	1.72	1.23	1.59	1.59	1.9	1.48	1.62	0.85	1.09	1.19	1.01
48-3-1	1.27	1.61	-	1.38	-	-	-	1.72	-	-	-	1.25
48-3-2	1.31	1.51	1.33	1.36	1.66	1.55	1.35	1.52	1.27	1.04	1.03	1.12

Table 7 Summary of results

Specimen	Description	Experiment			FE Analysis		
		Shear (kN)	% Increase	Failure Mode	Shear (kN)	% Increase	Failure Mode
24-3-2	No CFRP (Control)	467	0 %	Diagonal Tension	480	0 %	Diagonal Tension
24-3-5	1 Layer, 5''@10'' (Laminate B)	645	38 %	Rupture of CFRP	654	36 %	Rupture of CFRP
48-3-1	No CFRP (Control)	654	0 %	Stopped Loading	818	0 %	Diagonal Tension
48-3-2	1 Layer, 10''@20'' (Laminate A)	1005	54 %	Rupture of CFRP	1130	38 %	Rupture of CFRP

geometry and reinforcement. In case of group 1, the shear cracks in both control beam (24-3-2) and retrofitted beam (24-3-5) are inclined at around 45 degrees as evident from Figs. 9 and 20 respectively. Whereas in group 2, the shear behavior is appreciably different as the main diagonal crack in the control beam (48-3-1) and retrofitted specimen (48-3-2) is inclined at around 30 degrees as shown in Figs. 25 and 35, respectively. The inclination of cracks and their widths has significant effect on the de-bonding behavior of the CFRP strips.

With more cracks inclination, the length of crack passing CFRP strips increases which creates higher strains. Similarly, with the increase in crack width as the shear load increases, higher strains were developed in CFRP strips. Considering these observations, it has been found that the assumed contact technique used in this paper of CFRP in presence of anchors gives reasonably good results both in terms of ultimate shear capacity and failure modes as summarized in Table 7.

5.2 Evaluation of CFRP material and geometric property

Two different types of laminates A and B are considered in this study to investigate the effect of CFRP material and geometric properties on modeling and verifications of the shear strength of CFRP strips with anchors. Laminate A has higher modulus of elasticity whereas laminate B has around 35 percent less elastic modulus. In addition, the width and thickness of both the laminates are different. These properties have shown significant effect on crack pattern in CFRP strips. The FE prediction of crack pattern and location with respect to CFRP is found to be in good agreement with results obtained from experiments.

5.3 Evaluation of CFRP spacing and number of anchors

Different CFRP strip spacing and number of anchors

depending on the width of CFRP strip has been considered as detailed in Table 4 to evaluate the effect of spacing and number of anchors on the shear behavior of RC beams. It is established that if anchorage of CFRP strip is adequate and stronger than the strength of CFRP strips, then the failure occurs by CFRP rupture.

6. Results summary

Results of individual components obtained from ACI equations, experiments and the FE analysis are tabulated in Table 5.

Comparison of normalized results obtained from ACI equations, experiments and the FE analysis are tabulated in Table 6.

It can be observed from the comparative study in Table 6 that the ratio of the values of each shear resisting component (concrete, steel, and CFRP) in all beams between the experiment and the FEM are higher than the values obtained by the ACI. The results show that the ACI underestimated the shear strength of RC beams strengthened by CFRPs. However, the ratios between the FE results and experiments are close and in very good agreements, which shows the capability of FE to predict the shear capacity. The overall percentage increase in shear capacity due to CFRP and failure mode of each beam is observed and presented in Table 7.

7. Conclusions and future work

In this study, the behavior of reinforced concrete beams strengthened with externally bonded CFRP strips with special anchors has been investigated numerically. First, the criteria for advanced FE model for each component of beam shear resistance (concrete, CFRP and steel) is presented and its adequacy is demonstrated by comparing FE analysis results for each component with experimental values. Based on the assumption and the results of this study, the following conclusions are drawn:

- Bond interaction between concrete and CFRP plays an important role in overall shear deformation behavior and ultimate shear capacity. In normal CFRP strengthening without CFRP anchors, a perfect or hard cohesive bond can overestimate the shear capacity. But as demonstrated in this study with proper anchor details and its development length along with suitable epoxy between CFRP and concrete, interaction between CFRP and concrete can be considered as “hard dry” cohesive bond to appropriately simplify modelling and simulation of the anchored CFRP strips. This assumption is only suitable for the cases where failure is through CFRP rupture and not by de-bonding failure which can only be ensured through proper anchor details.
- The bond between concrete and steel is assumed to be perfect through embedment technique available in ABAQUS and it is found that this modelling assumption gives fairly good results but on the higher side as compared to experimental values. The possible reason can be due to the strong bond between steel and

concrete which made the results in slightly higher shear capacity. Thus further research is needed on the effect of different level of bond strengths between steel and concrete for further refinement. In addition, utilization of bond-slip model can be investigated.

- The topmost conclusion of this study is that proper material models and interaction between different components are decisive to appropriately simulate the shear behavior of reinforced concrete beam strengthen with CFRP. Further research work is needed to verify the post-peak behavior of CFRP strengthen RC beams which essentially requires the precise and vigilant experimental test results

Acknowledgements

The support of the Department of Civil and Environmental Engineering at KFUPM is acknowledged and appreciated.

References

- ACI committee 318 (2014), 318-14: Building Code Requirements for Structural Concrete and Commentary.
- ACI Committee 440 (2008), 440.2R-08 Guide for the Design and Construction of Externally Bonded FRP Systems for Strengthening Concrete Structures.
- ACI Committee 446 (1997), Finite Element Analysis of Fracture in Concrete Structures, State-of-the-Art (No. ACI 446.3R-97).
- Bansal, P.P., Sharma, R. and Mehta, A. (2016), “Retrofitting of RC girders using pre-stressed CFRP sheets”, *Steel Compos. Struct.*, **20**(4), 833-849.
- Birtel, V. and Mark, P. (2006), “Parameterised finite element modelling of RC beam shear failure”, *2006 ABAQUS Users' Conference*, 95-108.
- Bocciarelli, M., Gambarelli, S., Nisticò, N., Pisani, MA. and Poggi, C. (2014), “Shear failure of RC elements strengthened with steel profiles and CFRP wraps”, *Compos. Part B: Eng.*, **67**, 9-21.
- Chen, G.M. (2010), “Behaviour and strength of RC beams shear-strengthened with externally bonded FRP reinforcement”, Department of Civil and Structural Engineering, The Hong Kong Polytechnic University, Hong Kong, China.
- De Borst, R., Remmers, J.J.C., Needleman, A. and Abellan, M.A. (2004), “Discrete vs. smeared crack models for concrete fracture”, *Int. J. Numer. Anal. Meth. Geomech.*, **28**(7-8), 583-607.
- Gambarelli, S., Nisticò, N. and Özboltb, J. (2014), “Numerical analysis of compressed concrete columns confined with CFRP: Microplane-based approach”, *Compos. Part B: Eng.*, **67**, 303-312.
- Kim, Y., Quinn, K., Satrom, N., Garcia, J., Sun, W., Ghannoum, WM. and Jirsa, J.O. (2011), “Shear strengthening of reinforced and prestressed concrete beams using carbon fiber reinforced polymer (CFRP) sheets and anchors”, Technical Report No. FHWA/TX-12/0-6306-1, Center for Transportation Research The University of Texas at Austin 1616 Guadalupe Street, Suite 4.202 Austin, TX 78701.
- Lee, J. and Fenves, G. (1998), “Plastic-damage model for cyclic loading of concrete structures”, *J. Eng. Mech.*, **124**(8), 892-900.
- Lima, M., Doh, J., Hadi, M.H. and Miller, D. (2016), “The effects of CFRP orientation on the strengthening of reinforced concrete structures”, *Struct. Des. Tall Spec. Build.*, **25**(15), 759-784.

- Lublinter, J., Oliver, J., Oller, S. and Oñate, E. (1989), "A plastic-damage model for concrete", *Int. J. Solid. Struct.*, **25**(3), 299-326.
- Nisticò, N., Özbolub, J. and Polimanti, G. (2016), "Modeling of reinforced concrete beams strengthened in shear with CFRP: Microplane-based approach", *Compos. Part B: Eng.*, **90**, 351-364.
- Mercan, B. (2011), "Modeling and behavior of prestressed concrete spandrel beams", Ph.D Thesis, University of Minnesota, Minneapolis and St. Paul, Minnesota.
- Nisticò, N., Özbolub, J. and Polimanti, G. (2016), "Modeling of reinforced concrete beams strengthened in shear with CFRP: Microplane-based approach", *Compos. Part B: Eng.*, **90**, 351-364.
- Otoom, O.F.A., Smith, S.T. and Foster, S.J. (2006), "Finite element modeling of FRP shear strengthened RC beams", *Proceedings of the 3rd International Conference on FRP Composites in Civil Engineering (CICE 2006)*, Miami, Florida, USA.
- Panjehpour, M., Ali, A.A.A. and Aznieta, F.N. (2014), "Energy absorption of reinforced concrete deep beams strengthened with CFRP sheet", *Steel Compos. Struct.*, **16**(5), 481-489.
- Smith, S.T., Otoom, O. and Foster, S.J. (2006), "Finite element modelling of RC beams strengthened in shear with FRP composites", *Proceedings of the 2nd International Fib Congress*, Naples, Italy, June.
- Simulia (2013), *Getting Started with Abaqus*, Keyword Edition.
- Tzoura, E. and Triantafillou, T.C. (2016), "Shear strengthening of reinforced concrete T-beams under cyclic loading with TRM or FRP jackets", *Mater. Struct.*, **49**, 17-28.
- Tsai, W.T. (1998), "Uniaxial compressional stress-strain relation of concrete", *J. Struct. Eng.*, **114**(9), 2133-2136.
- Yang, Z.J. and Chen, J.F. (2005), "Finite element modelling of multiple cohesive discrete crack propagation in reinforced concrete beams", *Eng. Fract. Mech.*, **72**(14), 2280-97.
- Yang, Z.J. and Chen, J.F. (2004), "Fully automatic modelling of cohesive discrete crack propagation in concrete beams using local arc-length methods", *Int. J. Solid. Struct.*, **41**(3-4), 801-26.
- Yang, Z.J., Chen, J.F. and Proverbs, D. (2003), "Finite element modelling of concrete cover separation failure in FRP plated RC beams", *Constr. Build. Mater.*, **17**(1), 3-13.